Pertanika J. Sci. & Technol. 26 (1): 391 - 408 (2018)

PERTANIKA JOURNALS

SCIENCE & TECHNOLOGY

Journal homepage: http://www.pertanika.upm.edu.my/

Monodispersed and Size-controllable Potassium Silicate Nanoparticles from Rice Straw Waste Produced Using a Flame-assisted Spray Pyrolysis

Asep Bayu Dani Nandiyanto[1]*, Rena Zaen[1], Rosi Oktiani[1], Ade Gafar Abdullah[2] and Ari Arifin Danuwijaya[3]

[1]Department of Chemistry, Universitas Pendidikan Indonesia, Jl. Dr. Setiabudi, Bandung 40154, Indonesia
[2]Department of Electro Technique, Universitas Pendidikan Indonesia, Jl. Dr. Setiabudi, Bandung 40154, Indonesia
[3]Department of English, Universitas Pendidikan Indonesia, Jl. Dr. Setiabudi, Bandung 40154, Indonesia

ABSTRACT

The purpose of this study was to demonstrate a facile method to produce monodispersed and size-controllable potassium silicate nanoparticles from rice straw waste. Different from other methods that use expensive raw chemicals, our method utilises rice straw waste as a source of silica that is cost-free and largely available. In the experimental procedure, rice straw waste was burned. Then, the burned rice straw waste was put into the alkaline extraction process (using potassium solution) and flame-assisted spray-pyrolysis apparatus system. To support the flame-assisted spray-pyrolysis, we utilised commercially available liquid petroleum gas as a fuel source for the flame combustion process. Experimental results showed that the prepared particles are monodispersed, spherical, and having sizes in the range of nanometer (from 20 to 80 nm). The fuel flow rate plays important role in controlling particle size in the final product. Increases in the fuel lead to the formation of larger particles. Since the present method can convert rice straw into useful and valuable potassium silica particles, further development of this study would give a positive impact for the reduction of rice straw waste emission.

Keywords: Aerosol process, controllable size,flame spray pyrolysis, growth particle, nucleation, potassium silicate, silica nanoparticles, spray drying

ARTICLE INFO

Article history:
Received: 25 April 2017
Accepted: 28 November 2017

E-mail addresses:
nandiyanto@upi.edu (Asep Bayu Dani Nandiyanto),
rena.zaen95@student.upi.edu (Rena Zaen),
rosioktiani@student.upi.edu (Rosi Oktiani),
ade_gaffar@upi.edu (Ade Gafar Abdullah),
aridanuwijaya@upi.edu (Ari Arifin Danuwijaya)
*Corresponding Author

INTRODUCTION

Potassium silicate is an attractive material used in a wide range of applications, specifically for fertiliser (Kikuchi, 1999). This material is also widely used due to its high stability, chemical

ISSN: 0128-7680

flexibility, and biocompatibility (Tokunaga, 1991). For example, as fertiliser, this material is effective for increasing the amounts of sugar and amino acid in plants, making them resistant to insects, pests, and diseases (Kikuchi, 1996). Potassium silicate is also used for improving quality of fruit in terms of taste, shape, and colour (Tokunaga, 1991).

To produce potassium silicate, many methods have been reported by several research teams (see Table 1) (Beneke & Lagaly, 1989; Rastsvetaeva, Aksenov, & Taroev, 2010; Novotny, Hoff, & Schuertz, 1993; Baghramyan, Sargsyan, & Harutyunyan, 2016; Tokunaga, 1991; Kikuchi, 1999). The method typically employed direct interaction and reaction between "silica source" and "potassium hydroxide". Potassium hydroxide acts as a potassium source and an agent for dissolving silica component from its originated source. Then, the dissolved silica component (typically as silicic acid ($Si(OH)_4$)) incorporates with potassium element to create crystal/ composite potassium silicate.

Table 1
Current reports on the production of potassium silicate material

Method	Materials	Result	References
Chemical treatment	Fly ash and KOH	Powder	Tokunaga (1991)
	SiO_2 and K_2O	Solution	Santmyers (1957)
	Waste bottle and KOH	Solution	Mori (2003)
	SiO_2 and KOH	Hydrated micropowder	Beneke & Lagaly (1989)
	Coal ash and KOH	Powder	Kikuchi (1999)
Hydrothermal reaction	Quartz sand and KOH	Solution	Novotny, Hoff, & Schuertz (1993)
	Ground diatomite and KOH (with microwave process)	Glass	Baghramyan, Sargsyan, & Harutyunyan (2016)

Beneke and Lagaly (1989) reported the production process using commercially available silica. Their process is effective to form potassium silicate particles with sizes in micrometer range. However, their particle sizes are broad and there is no information regarding control of particle size. Successful method using commercially available silica has been reported by Rastsvetaeva et al. (2010). Their method is effective to create unique crystal. However, their method is complicated as it utilises extreme process condition [e.g., high pressure (up to 1000 atm)] and time-consuming process. In addition, both the methods employed commercially available silica, which is impractical for practical uses since the price of these chemicals is typically expensive. As a consequence, the selling price of potassium silicate products is uncompetitive against other available products.

To against the use of above raw materials, Novotny et al. (1993) used silica quartz sand in the hydrothermal method. Mori (2003) reported the use of waste bottle, which is contacted with potassium hydroxide. Bagramyan et al. (2016) reported the production of potassium silicate from dissolving ground diatomite rock. They utilised microwave treatment to assist the heat treatment process. However, both methods are limited to the production of potassium silicate solution. There is no information on the possibility process for generating powder. Other papers

have been reported by Tokunaga (1991) and Kikuchi (1999), who used fly ash and coal ash as the silica sources, respectively. Although both the methods are effective for the production of potassium silicate particles, they did not report in detail about the physicochemical properties and characteristics of potassium silicate product.

Based on the above methods, several problems still persisted. Specifically, to the best of our knowledge, there is no information on how to create monodispersed and size-controllable potassium silicate nanoparticles in existence. Nanoparticles are required because these types of materials give better performance. The physicochemical properties of nanomaterial are different from that of bulk material. Control of particle size is also crucial since the size determines the material performance (Nandiyanto & Okuyama, 2011).

In our previous report, silica particles were successfully produced from rice straw waste (Nandiyanto et al., 2016b). In short, we used a combination of alkali and acid treatment for extracting and isolating silica from its originated source. Spherical and pure silica with sizes in the submicrometer range were produced. Although the combination of alkali and acid treatment is effective to create submicrometer silica particles, the production of potassium-embeded silica particles is typically difficult. Potassium and other inorganic components leach during the washing process (that is conducted in each step). This is the fundamental reason for why all papers related to such combination of alkali and acid treatment always created pure silica material (Kalapathy, Proctor, & Shultz, 2000; Zaky et al., 2008).

The purpose of this study was to demonstrate a facile technique to produce monodispersed and size-controllable potassium silicate nanoparticles from rice straw waste. Rice straw was selected because this material contains high amount of silica. Rice straw waste is also one of the largest agricultural wastes produced in large quantities but has not been used commercially (Fadhlulloh, Rahman, Nandiyanto, & Mudzakir, 2014; Permatasari, Sucahya, & Nandiyanto, 2016).

In the experimental procedure, rice straw waste was burned. Then, the burned rice straw waste was put into the alkaline extraction process (using potassium solution) and flame-assisted spray-pyrolysis apparatus system. While other methods utilise the acid precipitation method to precipitate silica-related material, our method uses flame-assisted spray-pyrolysis technique that is effective to generate particles with sizes in the nanometer range (Nandiyanto & Okuyama, 2011). To support the flame-assisted spray-pyrolysis method, we utilised commercially available liquid petroleum gas (LPG) as a fuel source for the flame burner as it is largely available. Therefore, the use of this LPG gives possibility for further scaling up process (Nandiyanto, Fadhlulloh, Rahman, & Mudzakir, 2016a).

Direct application of the flame-assisted spray-pyrolysis method to the alkaline-treated solution is also important for maintaining the existence of potassium in the final product. The flame-assisted spray-pyrolysis method is also prospective to produce agglomerate-free and pure particles in just a few of seconds (Karthikeyan et al., 1997). Further, this method has many advantages, including its low-cost production, easy-to-control particle size, simple processing, high-production yield, and ease of conversion to mass manufacturing (Nandiyanto & Okuyama, 2011).

Experimental results showed that the prepared particles are spherical with the sizes from 20 to 80 nm. We also varied the fuel flow rate in the pyrolysis process, which is effective to

control the particle size. In addition, since the product is generated from the rice straw waste which has been underutilised till the present day, further development of the present study would have a great positive impact for the reduction of rice straw waste emission and conversion of waste into useful and valuable products.

BASIC INFORMATION ON RICE STRAW AND FLAME-ASSISTED SPRAY-PYROLYSIS METHOD

What Happened with the Rice Straw?

Rice straw in the agricultural country raises environmental problems (van Soest, 2006). For example, Indonesian Statistic Bureau in 2015 recorded that the rice production was 75.36 million tons. The production of rice increases every year (see https://www.bps.go.id/brs/view/id/1271; accessed on 24 December 2016). This huge amount remains for waste problems that are about 12-15 tons of rice straw as a by-product. These abundant by-products are typically disposed of and burned in the rice field, contributing severe air pollution issues.

Rice straw is rich in silica, organic, and inorganic nutrients (see Table 2) (Minu, Jiby, & Kishore, 2012). The organic nutrients in the rice straw mainly contain cellulose (32-47%), hemicellulose (19-27%), lignin (5-24%), and ash (13-20%), (Zaky et al., 2008) whereas the inorganic component is mostly alkali and earth alkali. As the rice straw contains high amount of silica (specifically, rice straw ash can contain 60-80 wt% of silica) (Nandiyanto et al., 2016b), the price is low and the existence of this waste is abundant, and rice straw can be used as an alternative source for silica.

How to Isolate Silica from Rice Straw?

Figure 1 shows illustration mechanism for the isolation of silica from rice straw waste, in which the process requires at least three steps. The steps include the burning process, alkali treatment, and conversion of silicic acid into silica.

The first step is a burning process. Since most of the rice straw components are organic-related compounds (Zaky et al., 2008), burning rice straw allows increases in surface area and decreases in volume. Most of the organic components turn into carbon dioxide gas and some are turned into ash. Thus, the burning process plays an important role for enriching the percentage of silica.

Next, the second step is the alkali treatment that is used for converting silica component (embedded in the ash) into silicic acid ($Si(OH)_4$). Silicic acid is water-dissolved chemical. The solubility of silicic acid increases in the pH of higher than 10 (Kalapathy, Proctor, & Shultz, 2000). The optimum pH to get excellent extraction process is 12-13 (Minu, Jiby, & Kishore, 2012). In general, the alkali treatment involves the following reaction:

$$Si\text{-}O\text{-}Si + H_2O \rightarrow 2Si\text{-}OH$$

$$Si\text{-}OH + M^+ + OH^- \rightarrow Si\text{-}O\text{-}M^+ + H_2O$$

where M is the alkali component such as sodium and potassium.

The third step is the conversion process from silicic acid into silica (SiO_2). Many techniques can be applied for achieving this conversion process such as acid and heat treatment. In this study, although many papers have reported the possibility of the conversion process using acid precipitation process (Lu & Hsieh, 2012), we limited our process using the heat treatment. The heat treatment is selected because this method is better than the acid treatment for maintaining the inorganic element (potassium and other inorganic components usually leach during the washing process in the acid treatment).

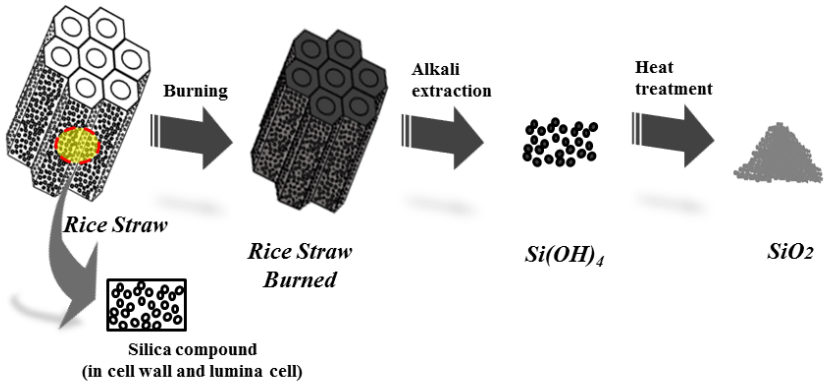

Figure 1. Illustration mechanism of the isolation of silica from the rice straw waste

Technical Information about Flame-assisted Spray-pyrolysis Method

Flame-assisted spray-pyrolysis method is a method for generating particles from liquid-phase solution via employment of the heat-shock treatment (Nandiyanto & Okuyama 2011). The production process involves generation of droplet from the initial solution. Next, the generated droplets are introduced to heat for evaporating solvent in the droplet (Chiang, Aroh, & Ehrman, 2012). Since heat-shock treatment is applied in the evaporation process, the final sizes of the produced particles are in the range of nano to submicrometer size (Nandiyanto & Okuyama, 2011).

Detailed information on the mechanism during the flame-assisted spray-pyrolysis method is shown in Figure 2. In general, the process (shown in Figure 2a) is started by generating droplets from liquid precursor. The generated droplets are then introduced into the reactor and put in direct contact with the flame. The flame itself is produced from the combustion of fuel with air. During the droplet travel, several steps occur (see Figure 2b), including solvent evaporation, droplet break-up, nucleation and growth process. The steps occur subsequently to form nanoparticles. In addition, the main important step for the successful production of nanoparticles is the droplet break-up step. This step can be achieved only due to the existence of heat-shock (that is achieved from the direct contact of droplet with the flame).

In addition, the flame process is conducted in the reactor system, as shown in Figure 2a. Thus, the heat in the process is typically maintained. The transfer of heat in the reactor is due to the heat radiation and convection that are gained from the combustion process of fuel and oxygen.

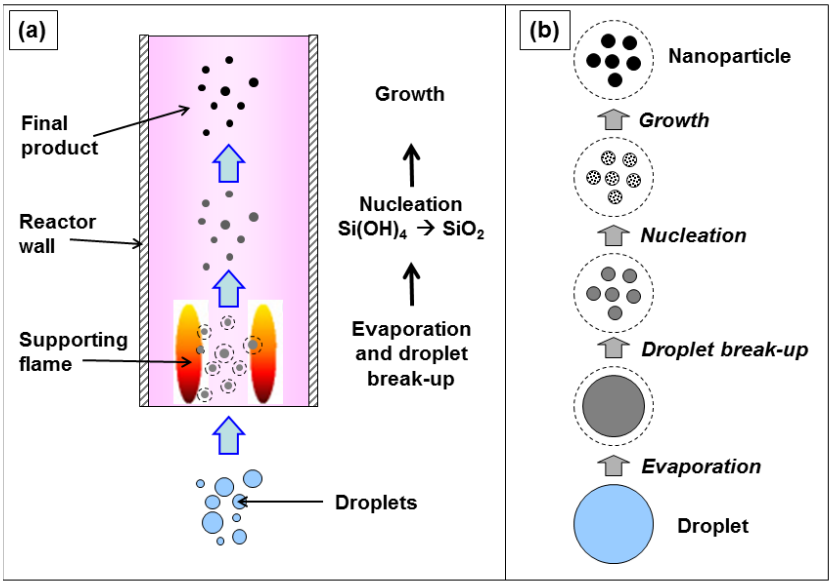

Figure 2. Illustration image of the particle formation mechanism. Figure (a) is the image for the particle travel phenomenon in the flame reactor, whereas Figure (b) is the particle formation mechanism

EXPERIMENTAL METHOD

Raw Materials

The following raw materials were used in this study: rice straw waste (rice field in Cimahi, Indonesia) and potassium hydroxide (KOH, 98%, PT. Bratachem, Indonesia). Rice straw was washed with ion-exchanged water, dried naturally for nine days, and then cut to get the size of about 1 cm.

Synthesis of Potassium Silicate Particles

Rice straw was heated in furnace at 973 K to produce rice straw ash in room condition. To ensure the conversion of organic material into ash, the heating process was maintained for about 7 hours in the furnace. Then, the rice straw ash was ground and put into the potassium hydroxide solution. The mixture was then stirred at 900 rpm and heated at 338 K for 2 hours. Next, the extraction solution was put into the flame-assisted spray-pyrolysis apparatus (equipped with commercial liquid petroleum gas (LPG; Pertamina) and flow of air to introduce droplets into flame apparatus).

In the flame-assisted spray-pyrolysis apparatus (see Figure 3), the system consisted of an ultrasonic nebuliser (NE112; Omron Corp., Japan, used for generating droplet with diameter of about 4.5 um; the ultrasonic nebuliser was equipped with cooling system and cyclone), a flame burner (used for drying as well as polymerising silica component), a flame reactor (stainless steel; diameter of 20 cm and total height of 50 cm), and a filter. The apparatus was also introduced by a flow of LPG (as a fuel source of flame burner) and flows of air. There are two types of air used in this study. One is carrier gas for introducing droplet from the

ultrasonic nebuliser to the flame reactor, and the other is total air that acts as an oxidiser combustion process in the burner. In this study, the flow of LPG in the flame-assisted spray pyrolysis was varied (in the range of 0.30 and 1.20 L/min), whereas the flows of air for the carrier and the oxidiser were fixed at 0.60 and 1.50 L/min, respectively. Based on our previous report (Nandiyanto, Fadhlulloh, Rahman, & Mudzakir, 2016a), fuel with gas flow rate below 0.30 L/min allows unstable flame, whereas fuel with gas flow rate exceeding 1.20 L/min gives impurities in the final product.

Characterisation

Chemical and functional groups, morphology, and particle size of potassium silicate particles were analysed using Transmission Electron Microscopy (TEM, JEOL JEM-1400, JEOL Ltd., Japan) and Fourier Transform Infrared (FTIR, FTIR-8400, Shimadzu Corp., Japan). To analyse the composition of gas, we used gas chromatography mass spectrometry (GC-MS, GCMS-QP2010 Ultra, Shimadzu Corp., Japan). To analyse the chemical component in the sample, we used several analysis methods including gravimetric (for analysing silica) and atomic absorption spectroscopy (AAS; Varian Spectra 240 FS, Varian Inc., US; for analysing metal oxide component).

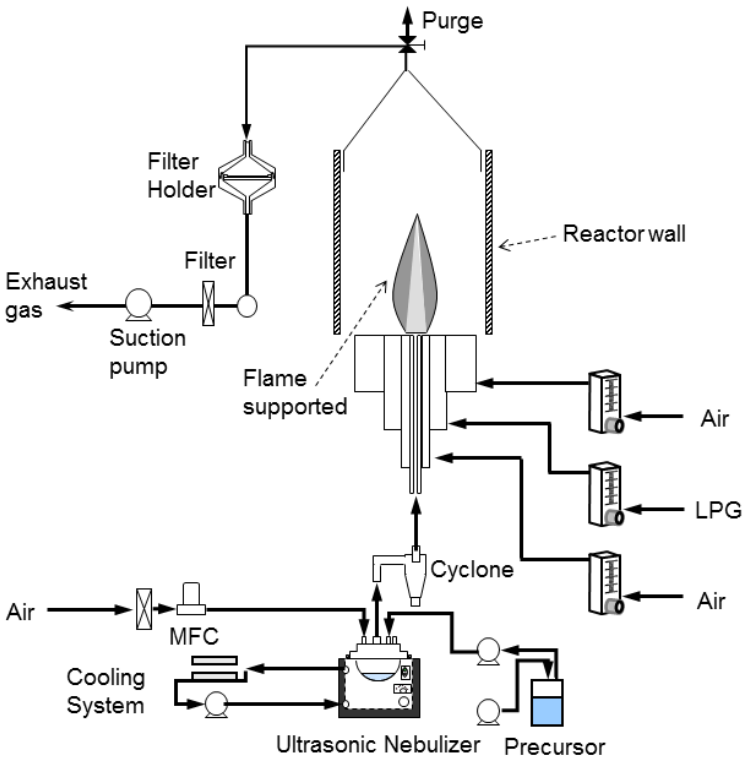

Figure 3. Illustration of the flame-assisted spray-pyrolysis apparatus. MFC is mass flow controller, and LPG is commercially available liquid petroleum gas

RESULTS AND DISCUSSION

Physicochemical Properties of Raw Materials

Table 2 shows the contents of silica and other component contained in the rice straw ash. The results identified that most of the components in the rice straw ash are silica, in which the amount of silica was 74.60%. Other components contained in the rice straw ash were ash, K_2O, CaO, MgO, Na_2O, Fe_2O_3, and Al_2O_3. As silica is the main component in the rice straw ash, we can conclude that rice straw is a potential source of silica material.

As a comparison for ensuring the effectiveness of our method for enriching silica, we added information on the chemical composition of rice straw adopted from the references (van Soest, 2006; Minu, Jiby, & Kishore, 2012; Zaky et al., 2008). We found that the concentration of silica increased from 13 to 74%. The increase in silica was followed by a great decrease in the composition of organic component. This revealed that most of the organic components decomposed into carbon dioxide, with some of them into ash. In addition, the table below presents information for the initial rice straw from the reference, while detailed information on the composition of silica in the initial raw straw will be given in our future work.

Table 2
The chemical contents of rice straw before and after the burning process

Composition	Before burning process	After burning process	
	Quantity (%)	Quantity (%)	Method
SiO_2	~13[a]	74.60	Gravimetric
Ash	13 – 20[c]	~ 5.00	
Oxide component		~ 12.00	AAS
K_2O	1.40 – 2.00[b]	9.06	AAS
CaO		1.87	AAS
MgO		1.48	AAS
Na_2O		0.45	AAS
Fe_2O_3		0.35	AAS
Al_2O_3		0.32	AAS
Organic component	~75		
Cellulose	32 – 47[c]		
Hemicellulose	19 – 27[c]		
Lignin	5 – 24[c]		
N	0.50 – 0.80[b]		
P_2O_5	0.16 – 0.27[b]		
S	0.05 – 0.10[b]		

Note: [a]Data were obtained from the reference (van Soest, 2006); [b]Data were obtained from the reference (Minu, Jiby, & Kishore, 2012). [c]Data were obtained from the reference (Zaky et al., 2008)

Figure 4 shows the GC-MS analysis results of the commercially available LPG used in this study. Based on the GC-MS analysis results, the LPG contained several combustible organic components including propane (58.90%), isobutane (18.35%), butane (22.26%), and 2-methyl

butane (0.48%). Since the component in the commercially available LPG is combustible, the LPG is prospective as a fuel source for flame-related process.

Based on the GC-MS results, complete combustion process is achieved if it only fits the following reaction:

$$LPG_{(g)} + 5.86\ O_{2(g)} \rightarrow 3.60\ CO_{2(g)} + 4.60\ H_2O$$

where LPG is the mixed gas containing propane (58.90%w), isobutane (18.35%w), butane (22.26%w) and 2-methyl butane (0.48%w). In simplification from the above chemical reaction, the mole ratio of oxygen and LPG must be 5.86. Thus, to completely combust 1 mole of LPG, the minimum number of oxygen is 5.86 mole.

Taking into account that the percentage of oxygen in the air is 21% and the densities of propane, iso butane, butane, 2-methyl butane, and oxygen are 0.55; 0.573; 0.573; 0.626; and 1.429 kg/m^3 (data obtained from www.chemicalbook.com; accessed on 24 December 2016), respectively, the minimum volume air required to reach a complete combustion of 1 L/min of LPG is about 10 L/min. In general, when using the flow rate of air of less than that value, the complete combustion cannot be obtained and the formation of carbon in the final product cannot be avoided as well.

Using the above correlation, the process was conducted using a gas carrier flow rate (air) of 0.45 L/min and a total air gas flow rate of 1.50 L/min, whereas the flow rate of LPG varied between 0.30 and 1.20 L/min, and the minimum total flow rate of air must be in the range between 3 and 12 L/min. Thus, we can conclude that the combustion process is supposed to give some carbon components in the product. Although the process must utilise higher flow rate of air, the use of higher rate of air can disturb the flame process. The flame is unstable and the possibility of fire to be ceased is high.

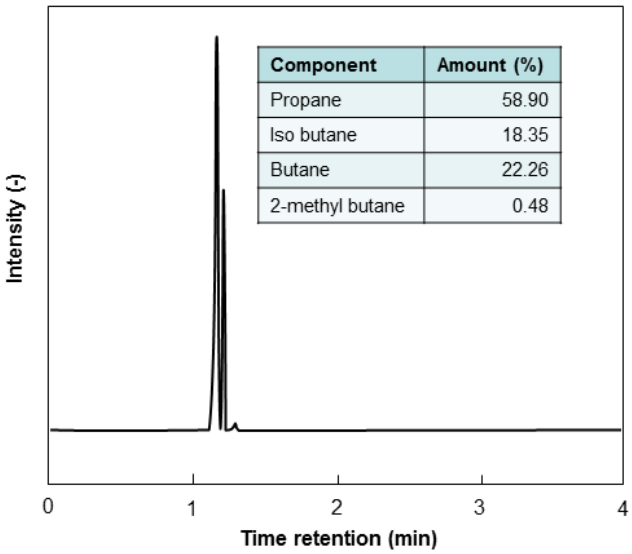

Figure 4. The GC-MS analysis result of commercially available LPG. The panelled table is the detailed information for the component in the LPG. The result was adopted from the following reference (Nandiyanto, Fadhlulloh, Rahman, & Mudzakir, 2016a)

Process Condition of Flame-assisted Spray-pyrolysis Apparatus: Effect of Fuel Flow Rate on the Reactor Temperature Profile

Figures 5a show the photograph image of flame for the production of particles. Figures 5a(i) and 5a(ii) are the images for the process conducted using 0.45 and 1.20 L/min of fuel flow rate, respectively. The images clearly reveal that the combustion process resulted in yellow flame. Some blue flames were formed only when conducting the experiments with the low rate of fuel. The higher rate for the fuel allowed the formation of greater fire with more yellow flame.

The existence of yellow flame is related to the production of incomplete combustion process. Indeed, it also indicates that carbon product will be created during the combustion process. To clarify the discussion about the carbon product, the following reaction happens:

$$LPG(g) + m\ O_{2(g)} \rightarrow n\ CO_{2(g)} + p\ CO_{(g)} + q\ C(s) + r\ H_2O$$

where LPG is the mixed gas containing propane (58.90%w), isobutane (18.35%w), butane (22.26%w), and 2-methyl butane (0.48%w). *m, n, p, q*, and *r* are, respectively, the reaction coefficient, depending on the availability of oxygen. In short, the more oxygen is supplied, the less values of p and q will be obtained. In general, in the constant air flow rate, the higher fuel flow rate allows less fuel molecules to contact and to be oxidised completely. Indeed, less oxidised fuel creates the decomposition of fuel without oxygen. As a consequence, carbon-related component is formed (the more value of q is formed) (Ribeiro & Pinho, 2004).

Figure 5b is the temperature distribution inside the reactor at a LPG flow rate of 0.90 L/min. We selected 0.9 L/min of LPG flow rate because the flame produced is typically stable. The blue flame was also found in this flow rate, while higher flow rate of LPG fuel would create more yellow flame in the process. To make discussion easier, the process temperature distribution was signed by the red colour, which was from transparent red to dark red. The figure clearly revealed that the temperature depended on the position from the flame reactor. The maximum temperature was reached in the specific position inside the flame (shown by the dark red area), whereas the farer from the flame resulted in the lower temperature (shown by the transparent red area). We also found that the temperature of wall in the reactor was relatively the same, which was in the range of 300 and 400°C.

In the centre of the reactor (shown as a dashed-and-dot line), the temperature was varied. This centre can be known as the main path of droplet travel because most of the droplets go through this line. In the position of 0 m distance, the temperature was between 100 and 300°C, in which, this was due to two reasons: the initial step for contacting fuel and oxygen (known as dark zone) and the interaction of flame with the droplet [Droplet evaporates some water (as a solvent)]. Indeed, this water cools the temperature because the evaporation of solvent absorbs some heat from its surrounding. The maximum temperature was reached at the distance between 0.125 and 0.15 m from the burner. The maximum temperature was about 700°C. Passing the position for the maximum temperature, the temperature decreased along the centre of the reactor to the outlet. Indeed, the decreases in the temperature were because the position was outside of the main flame (passing the **outermost zone**). In addition, the reactor wall temperature was almost the same in the range of 300 and 400°C due to the heat radiation (from the combustion process) and the force convection (in the wall itself).

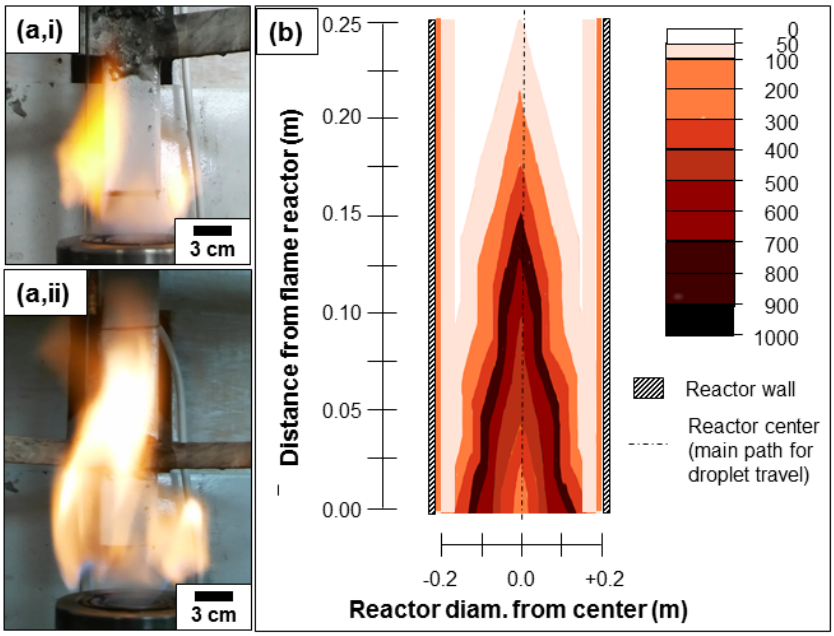

Figure 5. Photograph image of flame-supported pyrolysis method. Figures (a,i) and (a,ii) are the photograph images of flame produced using 0.45 and 1.20 L/min of LPG, respectively. Figure (b) is the reactor temperature profile at 0.90 L/min of LPG. All processes were conducted using a carrier gas flow rate (air) of 0.45 L/min, and a total air gas flow rate of 1.50 L/min

Figure 6 shows the temperature profile at the centre of reactor. The temperature was analysed using a conventional high-temperature-purpose thermocouple. To confirm the position of flame in the reactor, we added a photograph image of the flame (shown in the insert photograph image), and the position of the outer most zone was shown as a dashed line. As shown in the figure, the present flame is effective for heat-shock treatment that is required for droplet break-up phenomenon. The temperature increased extremely at the beginning of the process (from 0 to 10 cm distance from the burner). The temperature rose to more than 700°C. Then, the temperature increased gradually until it reached the maximum. After passing the fire interface line (see the dashed line), the temperature gradually decreased.

The maximum temperatures for 0.45; 0.60; 0.90; and 1.20 L/min of fuel flow rate were about 700; 785; 815; and 905°C, respectively. The increase in the fuel gas correlated with the generation of higher temperature. This is related to the number of breakage of fuel compound bond. The more broken fuel bond results in the more energy to be created.

During the flame, fire can be divided into several zones: dark zone, blue zone, luminous zone, and outermost zone. Dark zone (0-3 cm distance from the burner) is the zone when the reaction is started. The next zone is the blue zone, where the fuel has contacts with oxygen. Fuel compound's bond is broken and combined with oxygen. Some fuel compounds are radicalised. The third zone is the luminous zone (yellow zone), where the reaction continued from the blue zone. The radicalised fuel compounds combined with oxygen molecules further, breaking more bond. Indeed, higher temperature is created compared with the blue zone. The

final zone is the outermost zone. This zone is the hottest areas, with the temperature can take the maximum. However, passing this zone, the temperature drops significantly. Based on the experiments, the outermost zones for the burning process using 0.45; 0.60; 0.90; and 1.20 L/min of LPG fuel flow rate was about 10, 14, 16, and 17 cm distance from the burner, respectively.

Although the increase in the fuel gas is proportional to generate higher temperature, in which this temperature is crucial for evaporation and reaction process, the rate of fuel must be considered. The rate of fuel must be optimised and compared with the number of air flow rate. The ratio of fuel and air must be in the equal number in stoichiometry. Thus, to get a complete combustion process where all the fuel sources are converted into energy with carbon dioxide and water, the amount of air must be in excess. Otherwise, when using less amount of air, the product will have carbon impurities.

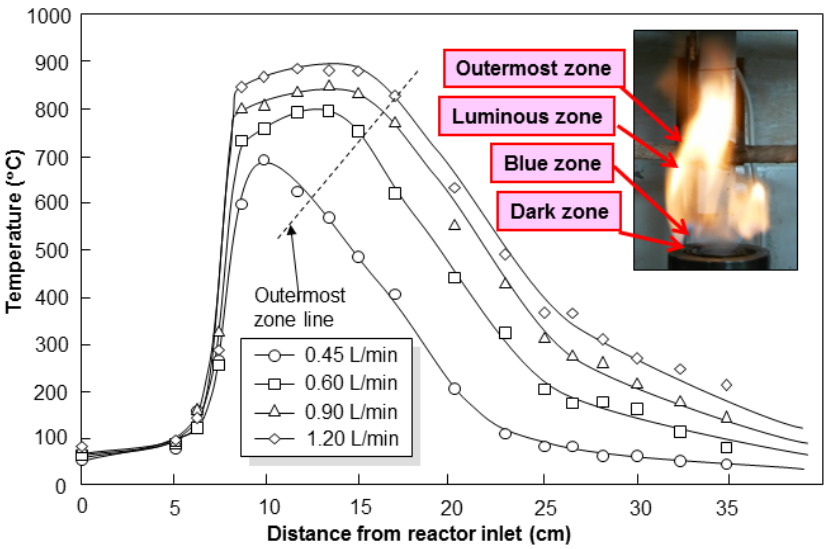

Figure 6. Reactor temperature profile at the centre of the reactor at various LPG fuel flow rates in the range of 0.45 and 1.20 L/min. The process was conducted using a carrier gas flow rate (air) of 0.45 L/min, and a total air gas flow rate of 1.50 L/min. Panelled figure was the photograph image of fire with information about the position of fire interface

Production of Potassium Silicate Nanoparticles with Controllable Size: Effects of LPG Flow Rate on the Final Particle Size

Figures 7a-c show the TEM analysis results of the particles prepared by using the flame-assisted spray-pyrolysis method. The image shows that the potassium silicate particles have a spherical morphology in the sizes of less than 100 nm (see Figure 7d).

As shown in Figure 7a, the particles in the sizes of about 25 nm were produced when the process conducted at an LPG fuel flow rate of 0.60 L/min. Then, the particles in the sizes of 75 nm were produced when the process was performed using the fuel flow rate of 0.90 L/min. These results give information that the fuel affects the final particle size.

A high magnification of TEM image in Figure 7c shows the spherical particle. The particle seems to have a composite structure due to the appearance of smaller white dots in the TEM image. The composed component as small dots (see arrow in the image) is from the potassium compound. However, to confirm our hypothesis regarding the existence of potassium compound as the small dot, we will do further analysis in our future work.

To confirm the effects of fuel flow rate on the final particle size, we varied the LPG fuel gas flow rate in the production process by using the flame-assisted spray-pyrolysis method. The result showed that the higher fuel gas flow rate allowed the production of larger particles (see Figure 7b). Less fuel flow rate did not result in the production of particles with several nanometres (see Figure 7a). Further, too slow results lead to unstable flame. Thus, the formation of particles was not successful.

In addition, based on the results above, the higher LPG flow rate can create larger particles. The main possible reason is the existence of carbon in the particle. The more fuel gas flow rate applied has a correlation with the existence of more carbon component as impurities in the final product.

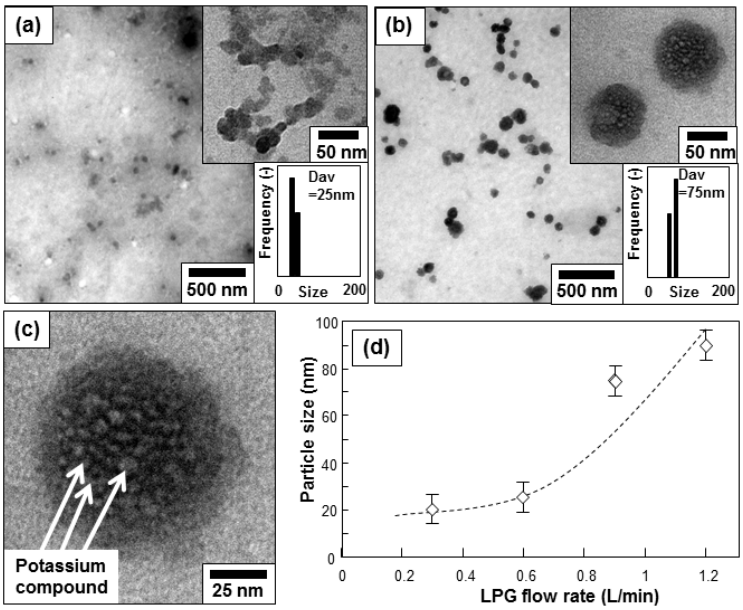

Figure 7. The TEM images of particles produced at various LPG flow rates. Figures (a) and (b) are the samples prepared at the LPG fuel flow rate of 0.60 and 0.90 L/min, respectively. Figure (c) is the high magnification of the TEM image of sample prepared at the fuel flow rate of 0.9 L/min. Figure (d) is the effect of LPG flow rate on the particle size. All the processes were conducted using a carrier gas flow rate (air) of 0.45 L/min, and a total air gas flow rate of 1.50 L/min

Figure 8 shows the FTIR analysis results of the flame spray-pyrolysed samples. In particular, the results showed almost similar absorption peaks and patterns for all the samples. The peak intensities were almost the same for all the samples, except for the peaks in the range of 2000-2100 and 2500-3000 cm^{-1} (see the dashed line area). Absorption peaks of silica-related

compound were identified, including the peaks at 806.25, 883.40, 1058.92, and 3194 cm^{-1} that ascribed to the existence of Si-O-Si symmetric stretching, Si-OH, Si-O-Si asymmetric stretching, and SiO-H, respectively. Further, FTIR also detected the peaks at 1128.36 and 1662.64 cm^{-1}, in which these belonged to Si-O-X (X = K, Si, atau H) stretching and K_2SiO_3, respectively. Detection of these potassium-related peaks strengthened our hypothesis that the present process is effective for maintaining potassium element in the product.

In addition to the above peaks, unique absorption peaks in the range of 2000-2100 and 2500-3000 cm^{-1} have different intensities for all the samples (as shown in the dashed line area in the figure). The intensities of the peaks increased with the increasing LPG fuel flow rate. The most different peak at in the range of 2000-2100 was obtained for the sample with 1.20 L/min of LPG flow rate. The appearance of these peaks corresponds to the existence of carbon-related component, which matches with our hypothesis (explained in Figure 4) and matches with our previous work (Nandiyanto, Fadhlulloh, Rahman, & Mudzakir, 2016a).

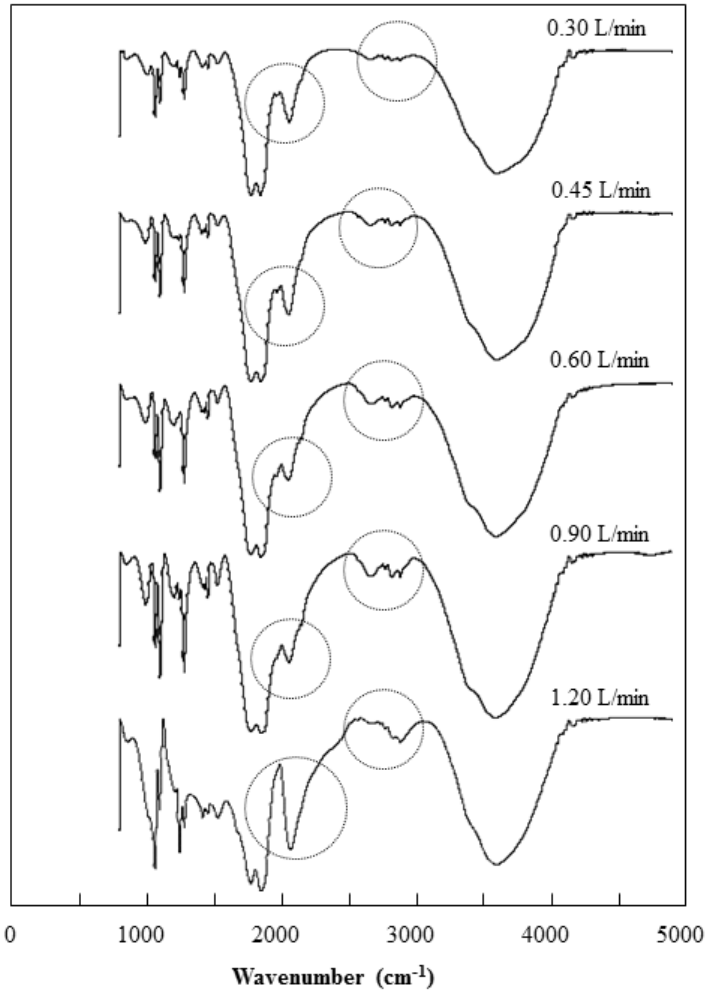

Figure 8. The FTIR analysis results of the samples produced at various LPG fuel flow rates in the range of 0.30 and 1.20 L/min. All the processes were conducted using a carrier gas flow rate (air) of 0.45 L/min, and a total air gas flow rate of 1.50 L/min

To ensure the peaks existed in the FTIR analysis, we presented a list of related peaks in comparison to the references (see Table 3) (Simonsen, Sønderby, Li, & Søgaard, 2009; Scarano, Bertarione, Spoto, Zecchina, & Arean, 2001; Cotton & Kraihanzel, 1962; Skoog & West, 1980; Nandiyanto et al., 2016b). As shown in the table, the peaks detected in the range of 2500 and 3000 cm^{-1} in Figure 8 are carbon-related material. The existence of carbon-related material is proportional with the flow rate of fuel. Indeed, in the constant flow rate of air, the higher flow rate of fuel correlated to the higher possibility to form carbon in the incomplete combustion process (Nandiyanto, Fadhlulloh, Rahman, & Mudzakir, 2016a).

Based on the FTIR data, the optimum condition to get potassium silicate particles is when applying process with less than 0.90 L/min of LPG fuel flow rate. Applying more than 0.90 L/min of LPG fuel rate would result in carbon component impurities in the particle.

Table 3
The FTIR spectra for silica and carbon-related material based on the references

Function Group	FTIR peak (cm^{-1})	Reference
Si-O-Si symmetric bending	461.34	Simonsen, Sønderby, Li, & Søgaard (2009)
Si-H	623	Simonsen, Sønderby, Li, & Søgaard (2009)
Si-O-Si symmetric stretching	795	Simonsen, Sønderby, Li, & Søgaard (2009)
Si-OH	895-880	Simonsen, Sønderby, Li, & Søgaard (2009)
Si-O-Si asymmetric stretching	1107	Simonsen, Sønderby, Li, & Søgaard (2009)
SiO-H	3400-3200	Simonsen, Sønderby, Li, & Søgaard (2009)
Si-O-X (X= K, Si, atau H) stretching	1100	Simonsen, Sønderby, Li, & Søgaard (2009)
K_2SiO_3	1625	Simonsen, Sønderby, Li, & Søgaard (2009)
Si-O stretching	1000-1200	Simonsen, Sønderby, Li, & Søgaard (2009)
Si-O bending	890-975	Simonsen, Sønderby, Li, & Søgaard (2009)
C-H (Alkanes)	2850-2970	Scarano, Bertarione, Spoto, Zecchina, & Arean (2001)
C-H (Alkenes)	3010-3095	Scarano, Bertarione, Spoto, Zecchina, & Arean (2001)
C-H (Alkynes)	3000	Scarano, Bertarione, Spoto, Zecchina, & Arean (2001)
C-H (aromatic rings)	3010-3100	Scarano, Bertarione, Spoto, Zecchina, & Arean (2001)
C-O	1050-1300	Cotton & Kraihanzel (1962)
C=O	1690-1760	Cotton & Kraihanzel (1962)
C-C	2100-2260	Cotton & Kraihanzel (1962)
C=C(alkenes)	1610-1680	Skoog & West (1980)
C-C(aromatic rings)	1500-1600	Skoog & West (1980)
C≡C(Alkynes)	2100-2260	Skoog & West (1980)

CONCLUSION

We have successfully demonstrated the technique to produce potassium silicate nanoparticles with controllable particle size (from 20 to 80 nm). This is different from other methods that used expensive raw chemicals, in this study, rice straw waste was used as a source of silica that is relatively low in price and largely available. To assist the production of nanoparticles, we used flame-assisted spray-pyrolysis method that utilised LPG as the fuel source for burner. We found that the prepared particles are spherical in sizes of nanometer range. To control the particle size, we found that managing fuel flow rate is the best option. In addition to the successful production of potassium silicate nanoparticles, since the product is generated from the rice straw waste that has remained underutilised until now, a further development of the present study would have a great positive impact for the reduction of rice straw waste emission and conversion of waste into useful and valuable products.

ACKNOWLEDGEMENT

Authors would like to acknowledge RISTEK DIKTI for supporting the research fund. Authors would also like to thank Novie Permatasari and Transmissia Noviska Sucahya for the assistance and support given in conducting this research.

REFERENCES

Baghramyan, V., Sargsyan, A., & Harutyunyan, V. (2016). Synthesis sodium, potassium silicates for thermoregulating coatings space vehicles by microwave method. *Journal of Armenia, 1*(68), 2016.

Beneke, K., & Lagaly, G. (1989). A hydrated potassium layer silicate and its crystalline silicic acid. *American Mineralogist, 74*(1-2), 224-229.

BPS. (2016). *Produksi padi tahun 2015 naik 6,37 persen*. Retrieved December, 2016, from https://www.bps.go.id/brs/view/id/1271

Chiang, C. Y., Aroh, K., & Ehrman, S. H. (2012). Copper oxide nanoparticle made by flame spray pyrolysis for photoelectrochemical water splitting–Part I. CuO nanoparticle preparation. *International Journal of Hydrogen Energy, 37*(6), 4871-4879.

Cotton, F. A., & Kraihanzel, C. S. (1962). Vibrational spectra and bonding in metal carbonyls. I. Infrared spectra of phosphine-substituted group VI carbonyls in the CO stretching region. *Journal of the American Chemical Society, 84*(23), 4432-4438.

Fadhlulloh, M. A., Rahman, T., Nandiyanto, A. B. D., & Mudzakir, A. (2014). Review tentang sintesis SiO2 Nanopartikel. *Jurnal Integrasi Proses, 5*(1), 30-45.

Kalapathy, U., Proctor, A., & Shultz, J. (2000). A simple method for production of pure silica from rice hull ash. *Bioresource Technology, 73*(3), 257-262.

Karthikeyan, J., Berndt, C. C., Tikkanen, J., Wang, J. Y., King, A. H., & Herman, H. (1997). Nanomaterial powders and deposits prepared by flame spray processing of liquid precursors. *Nanostructured Materials, 8*(1), 61-74.

Kikuchi, R. (1999). Application of coal ash to environmental improvement: Transformation into zeolite, potassium fertilizer, and FGD absorbent. *Resources, Conservation and Recycling, 27*(4), 333-346.

Lu, P., & Hsieh, Y. L. (2012). Preparation and characterization of cellulose nanocrystals from rice straw. *Carbohydrate Polymers, 87*(1), 564-573.

Minu, K., Jiby, K. K., & Kishore, V. V. N. (2012). Isolation and purification of lignin and silica from the black liquor generated during the production of bioethanol from rice straw. *Biomass and Bioenergy, 39*, 210-217.

Mori, H. (2003). Extraction of silicon dioxide from waste colored glasses by alkali fusion using potassium hydroxide. *Journal of Materials Science, 38*(16), 3461-3468.

Nandiyanto, A. B. D., Fadhlulloh, M. A., Rahman, T., & Mudzakir, A. (2016a). Synthesis of carbon nanoparticles from commercially available liquified petroleum gas. IOP Conference Series: *Materials Science and Engineering, 128*(1), 012042.

Nandiyanto, A. B. D., Rahman, T., Fadhlulloh, M. A., Abdullah, A. G., Hamidah, I., & Mulyanti, B. (2016b). Synthesis of silica particles from rice straw waste using a simple extraction method. I*OP Conference Series: Materials Science and Engineering, 128*(1), 012040.

Nandiyanto, A. B. D., & Okuyama, K. (2011). Progress in developing spray-drying methods for the production of controlled morphology particles: From the nanometer to submicrometer size ranges. *Advanced Powder Technology, 22*(1), 1-19.

Novotny, R., Hoff, A., & Schuertz, J. (1993). *U.S. Patent No. 5,238,668*. Washington, DC: U.S. Patent and Trademark Office.

Permatasari, N., Sucahya, T. N., & Nandiyanto, A. B. D. (2016). Review: Agricultural wastes as a source of silica material. *Indonesian Journal of Science and Technology, 1*(1) 82-106.

Rastsvetaeva, R. K., Aksenov, S. M., & Taroev, V. K. (2010). Crystal structures of endotaxic phases in europium potassium silicate having a pellyite unit cell. *Crystallography Reports, 55*(6), 1041-1049.

Ribeiro, L., & Pinho, C. (2004). Generic behaviour of propane combustion in fluidized beds. *Chemical Engineering Research and Design, 82*(12), 1597-1603.

Santmyers, D. (1957). *U.S. Patent No. 2,784,060*. Washington, DC: U.S. Patent and Trademark Office.

Scarano, D., Bertarione, S., Spoto, G., Zecchina, A., & Arean, C. O. (2001). FTIR spectroscopy of hydrogen, carbon monoxide, and methane adsorbed and co-adsorbed on zinc oxide. *Thin Solid Films, 400*(1), 50-55.

Skoog, D. A., & West, D. M. (1980). *Principles of instrumental analysis* (Vol. 158). Philadelphia: Saunders College.

Simonsen, M. E., Sønderby, C., Li, Z., & Søgaard, E. G. (2009). XPS and FT-IR investigation of silicate polymers. *Journal of Materials Science, 44*(8), 2079-2088.

Tokunaga, Y. (1991). Potassium silicate: a slow-release potassium fertilizer. *Nutrient Cycling in Agroecosystems, 30*(1), 55-59.

van Soest, P. J. (2006). Rice straw, the role of silica and treatments to improve quality. *Animal Feed Science and Technology, 130*(3), 137-171.

Zaky, R. R., Hessien, M. M., El-Midany, A. A., Khedr, M. H., Abdel-Aal, E. A., & El-Barawy, K. A. (2008). Preparation of silica nanoparticles from semi-burned rice straw ash. *Powder Technology, 185*(1), 31-35.